INTERNATIONAL JOURNAL FOR NUMERICAL METHODS IN FLUIDS, VOL. 15, 975–984 (1992)

A PC-BASED SYSTEM FOR MODELLING OF CONVECTION IN ENCLOSURES ON THE BASIS OF THE NAVIER–STOKES EQUATIONS

M. K. ERMAKOV, V. L. GRYAZNOV, S. A. NIKITIN, D. S. PAVLOVSKY AND V. I. POLEZHAEV

Institute for Problems in Mechanics, Russian Academy of Sciences, Prospect Vernadskogo 101, 117526 Moscow, Russia

SUMMARY

A PC-based system for modelling of convection in enclosures on the basis of the Navier–Stokes equations is described and a number of test results are given. New examples of mixed convection in a square chamber and thermal convection in ordinary and porous (isotropic and anisotropic) vertical layers are presented which may be of interest in civil and building engineering.

KEY WORDS Natural convection Forced convection Porous medium Numerical modelling CFD package

1. INTRODUCTION

Since the first papers on modelling of convection in enclosures on the basis of the Navier–Stokes equations, most of the main thermal convection problems have been solved, i.e. vertical layers with side heating,[1] enclosures with bottom heating and inclined,[2] unsteady problems with heat supply,[3] thermal and thermoconcentrational convection in horizontal layers with side heating[4,5] and the problem of transition from laminar to turbulent convection in vertical layers.[6] Similar problems have been solved also for convection in porous layers[7,8] (see additional references e.g. in Reference 9). Different kinds of packages for solving CFD problems on the basis of the Navier–Stokes equations with the help of finite difference and finite element methods are now available.[10–12] However, for a number of civil and building engineering problems it is possible to produce simpler and more user-friendly software for powerful personal computers which will be an additional tool for engineering handbooks (see e.g. Reference 13). This paper contains a description of one version of such a system: statement of problem, mathematical model, structure of system, tests and engineering results.

2. MATHEMATICAL MODEL

2.1. Ordinary media

For ordinary media the presented system is based on the two-dimensional unsteady Navier–Stokes equations for thermoconcentrational (double-diffusion) convection. The angle of inclination of the body force and the temporal behaviour (rotation, vibration) are taken into account. For the modelling of the thermoconcentrational convection, the Navier–Stokes equations with the Boussinesq approximation in a flat rectangular region of length L and height H are

0271-2091/92/210975-10$10.00 *Received March 1992*

used. The origin of the Cartesian system of co-ordinates (x, y) is the bottom left corner of the region. The governing equations are

$$\frac{\partial u}{\partial t}+u\frac{\partial u}{\partial x}+v\frac{\partial u}{\partial y}=-\frac{1}{\rho}\frac{\partial p}{\partial x}+\frac{\mu}{\rho}\Delta u+g_x(t)\left(\frac{\partial \rho}{\partial T}(T-T_0)+\frac{\partial \rho}{\partial C}(C-C_0)\right)\Big/\rho, \tag{1}$$

$$\frac{\partial v}{\partial t}+u\frac{\partial v}{\partial x}+v\frac{\partial v}{\partial y}=-\frac{1}{\rho}\frac{\partial p}{\partial y}+\frac{\mu}{\rho}\Delta v+g_y(t)\left(\frac{\partial \rho}{\partial T}(T-T_0)+\frac{\partial \rho}{\partial C}(C-C_0)\right)\Big/\rho, \tag{2}$$

$$\frac{\partial u}{\partial x}+\frac{\partial v}{\partial y}=0, \tag{3}$$

$$\frac{\partial T}{\partial t}+u\frac{\partial T}{\partial x}+v\frac{\partial T}{\partial y}=\alpha\Delta T, \tag{4}$$

$$\frac{\partial C}{\partial t}+u\frac{\partial C}{\partial x}+v\frac{\partial C}{\partial y}=D\Delta C, \tag{5}$$

where t is the time, (u, v) is the velocity vector, p is the pressure, T is the temperature, C is the impurity concentration, μ is the dynamic viscosity, ρ is the density, α is the thermal diffusivity and D is the diffusivity.

The fluid is initially motionless (velocity equal to zero) and the temperature and impurity concentration are either uniform or linearly distributed in any direction.

Different kinds of boundary conditions may be used. The normal component of velocity is given on every boundary. For the tangential component of velocity, u_s, the condition may be either of the first kind, $u_s=U_0$ (rigid wall), or of the second kind,

$$\mu\frac{\partial u_s}{\partial n}=\frac{\partial \sigma}{\partial T}\frac{\partial T}{\partial s}+\frac{\partial \sigma}{\partial C}\frac{\partial C}{\partial s},$$

where σ is the surface tension (free surface). For the temperature and concentration, boundary conditions of the first, second or third kind may be used.

The density of the binary liquid and the surface tension are given as linear functions of concentration and temperature:

$$\rho=\rho_0\left(1-\frac{1}{\rho}\frac{\partial \rho}{\partial T}(T-T_0)+\frac{1}{\rho}\frac{\partial \rho}{\partial C}(C-C_0)\right),$$

$$\sigma=\sigma_0+\frac{\partial \sigma}{\partial T}(T-T_0)+\frac{\partial \sigma}{\partial C}(C-C_0).$$

The components of the microacceleration vector, $g_x(t)$ and $g_y(t)$, can be written in the form

$$g_x(t)=g_{x0}+[g_s+g_t\sin(\Omega_1 t)]\sin(\Omega_2 t+\varphi_0),$$

$$g_y(t)=g_{y0}+[g_s+g_t\sin(\Omega_1 t)]\cos(\Omega_2 t+\varphi_0),$$

where g_{x0} and g_{y0} are the components of the constant microacceleration, g_s and g_t are constant and variable components respectively due to rotation in the case where it exists, Ω_1 and Ω_2 are the frequencies of vibration and rotation respectively and φ_0 is the initial angle of inclination. This type of representation includes the principal cases of space and temporal variation of the microacceleration vector.

These equations and boundary conditions may be non-dimensionalized with respect to any scales for time, length, velocity, etc. The principal non-dimensional parameters governing the behaviour of the system are: L/H, the aspect ratio; $Pr=\mu/\rho\alpha$, the Prandtl number; $Sc=\mu/\rho D$, the Schmidt number;

$$Gr_x=g_x\frac{1}{\rho}\frac{\partial\rho}{\partial T}\Delta T\,H^3\bigg/\left(\frac{\mu}{\rho}\right)^2,\qquad Gr_y=g_y\frac{1}{\rho}\frac{\partial\rho}{\partial T}\Delta T\,H^3\bigg/\left(\frac{\mu}{\rho}\right)^2,$$

the thermal Grashof numbers;

$$Gr_{xc}=g_x\frac{1}{\rho}\frac{\partial\rho}{\partial C}\Delta C\,H^3\bigg/\left(\frac{\mu}{\rho}\right)^2,\qquad Gr_{yc}=g_y\frac{1}{\rho}\frac{\partial\rho}{\partial T}\Delta C\,H^3\bigg/\left(\frac{\mu}{\rho}\right)^2,$$

the concentrational Grashof numbers; $Re=U_0H/(\mu/\rho)$, the Reynolds number; $Ma=(\partial\sigma/\partial T)\Delta T\,H/\mu\alpha$, the thermal Marangoni number; $Ma_c=(\partial\sigma/\partial C)\Delta C\,H/\mu D$, the concentrational Marangoni number.

2.2. Porous media

Darcy's law and the Boussinesq approximation for isotropic and anisotropic media are used for convection in permeable porous media (thermal insulation). In this case special definitions of the Rayleigh number $Ra^*=g\,Lk_y\Delta T/\nu\alpha^*$ and the anisotropic coefficient K_x/K_y are also used (α^* is the thermal diffusivity of anisotropic media).

$$\frac{1}{\rho}\frac{\partial p}{\partial x}+\frac{\nu}{k_x}u+g_x\frac{1}{\rho}\frac{\partial\rho}{\partial T}(T-T_0)=0, \tag{6}$$

$$\frac{1}{\rho}\frac{\partial p}{\partial y}+\frac{\nu}{k_y}v+g_y\frac{1}{\rho}\frac{\partial\rho}{\partial T}(T-T_0)=0, \tag{7}$$

$$\frac{\partial u}{\partial x}+\frac{\partial v}{\partial y}=0, \tag{8}$$

$$(\rho c_p)_m\frac{\partial T}{\partial t}+(\rho\,c_p)_f\left(u\frac{\partial T}{\partial x}+v\frac{\partial T}{\partial y}\right)=\lambda_m\left(\frac{\partial^2T}{\partial x^2}+\frac{\partial^2T}{\partial x^2}\right), \tag{9}$$

where c_p is the specific heat capacity and λ is the thermal conductivity; index 'm' corresponds to the fluid-saturated porous matrix and index 'f' to the fluid.

2.3. Numerical method

Equations (1)–(5) for ordinary media and (6)–(9) for porous media are solved by the finite difference method. The non-uniform staggered MAC mesh is used for space approximation. An explicit variant of the projection method proposed by Chorin and Temam[14] is applied for time approximation of the momentum equations (1) and (2). The temperature and concentration transport equations (4), (5) and (9) are solved by the DuFort–Frankel leapfrog method. The Poisson equation for pressure is obtained from (1), (2) or (6), (7). This equation with Neumann boundary conditions is solved iteratively by the SOR method with the optimum relaxation factor determined experimentally. The convective terms in the transport equations are approximated by central or 'upwind' differences. The finite difference approximations of the boundary conditions are of second-order accuracy.

The implicit scheme for ordinary media in the vorticity–streamfunction formulation[10] is also used. The alternating direction implicit (ADI) method is employed for the vorticity, temperature and concentration equations. The iterative ADI method or Fourier series method is employed for the streamfunction equation. The implicit scheme allows us to increase the time step of calculations and to accelerate the problem solving.

3. STRUCTURE OF PC-BASED SYSTEM

The described system is planned as a flexible and convenient software tool for solving different applications on the basis of the unsteady Navier–Stokes equations. Special attention is paid to creating a convenient user interface and to developing possibilities for numerical results visualization.

The common structure of the system is shown in Figure 1. The system supports three main groups of functions: problem statement, input control parameters (preprocessor); solving of the problem (solver); additional results processing, data visualization, conversion of data to formats of other software packages for analysis and plotter drawing (postprocessor).

All parts of the system work under the control of the common graphical shell in the united user medium. The software shell is based on the use of pull-down menus, hot keys, multiwindow graphical interfacing and mouse control. There are detailed help panels explaining the possible input selections and defaults to ease user input requirements.

The system is based on two software parts: a control part and an application part. The control part supports the software shell, common parameters input, package control, common functions, additional results processing and visualization. The application part contains problem parameters input, solver and data access procedures for additional results processing and visualization. Such a structure of the system allows one to focus on a required application. The applications are restricted by the prescribed shape of the region.

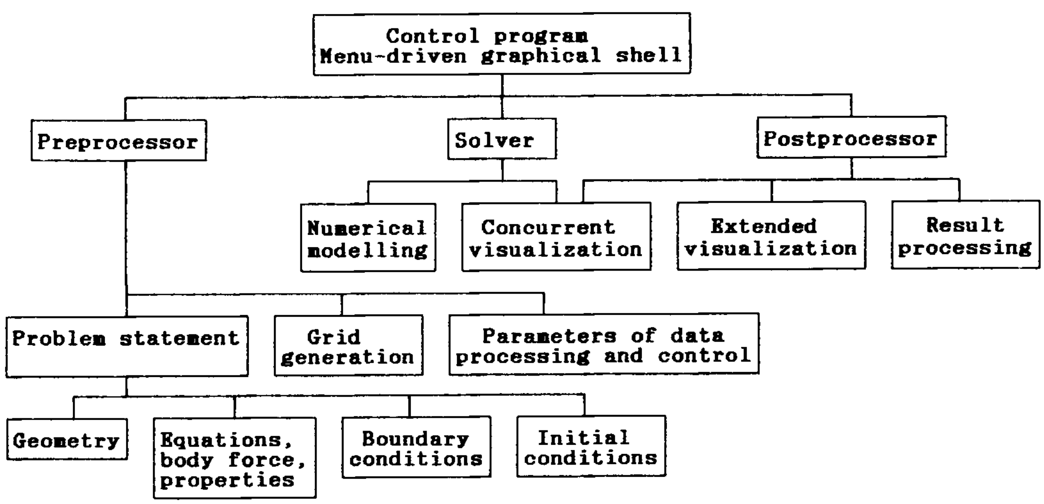

Figure 1. Common structure of PC-based system for modelling of convection on the basis of the Navier–Stokes equations

The preprocessor has the following important possibilities:

(i) formulation of the physical problem, including size of region, number of equations, initial and boundary conditions, physical properties of the fluid; it is also possible to impose the time dependence of the body force value and direction
(ii) assigning parameters of the finite difference solver, including number of grid nodes along each direction, approximation method for the convective members of the equations, method for time step calculation, scales of physical quantities, time of solving
(iii) grid generation
(iv) task control and several service functions, including loading and saving task status, parameters input from a file, system set-up, parameters check.

While the problem is solving, the following possibilities of concurrent visualization may be used:

(i) displaying the current values at some points and in a subregion
(ii) plotting the flow history at some points and in a subregion
(iii) displaying the isolines of temperature, impurity concentration or streamfunction.

The extended visualization of the postprocessor has additional tools for results presentation:

(i) drawing the sections of the fields in any direction
(ii) visualization of the flow structure by 'particle' tracks.

The described system works on an IBM-compatible PC with 640 kbyte RAM, mathematical coprocessor and EGA/VGA monitor. DOS 3.0 or higher is required. The numerical grid may contain up to 10000 nodes.

4. TEST EXAMPLES

A number of test examples described in Reference 15 have been solved: the de Vahl Davis test,[16] the GAMM test[17] and tests of our previous calculations mentioned above.[1–8,10] i.e. double diffusion, Marangoni convection, etc.

The first problem is natural convection of air ($Pr=0{\cdot}71$) in a square enclosure with isothermal side boundaries and insulated horizontal walls. Our solution of this problem was obtained at a Rayleigh number $Ra=Gr\times Pr=10^5$ using a 21×21 uniform mesh. The maximum value of the stream function is $\psi_{max}=9{\cdot}907$ for the explicit scheme and $\psi_{max}=8{\cdot}705$ for the implicit scheme. The test result of Reference 16 is $\psi_{max}=9{\cdot}612$, the discrepancy with our results therefore being about 3% and 9% respectively. The time taken on an IBM PC/387 for the modelling of the described problem (computation up to a non-dimensional physical time of 0·1) is approximately 100 for the explicit scheme and 25 for the implicit scheme.

The second problem is convection in a horizontal layer of a melt with side heating. The aspect ratio is 4:1, $Pr=0$ and the mesh is 101×26 at two Grashof numbers, $Gr=2\times 10^4$ and 4×10^4, in accordance with the GAMM test.[17] The corresponding values of ψ_{max} are 0·4066 (test result $\psi_{max}=0{\cdot}4155$) and 0·4146 (test result $\psi_{max}=0{\cdot}4167$), the discrepancy being 2% and 0·5% respectively. The flow structures for these cases are shown in Figure 2 by streamfunction isolines.

Figure 3 shows an example of our solution of another classical problem (the Rayleigh–Benard problem) for convection in a horizontal layer with bottom heating (lateral boundaries are adiabatic). The aspect ratio is 6:1, the mesh 60×11, $Pr=1$ and $Ra=10^4$, which corresponds to

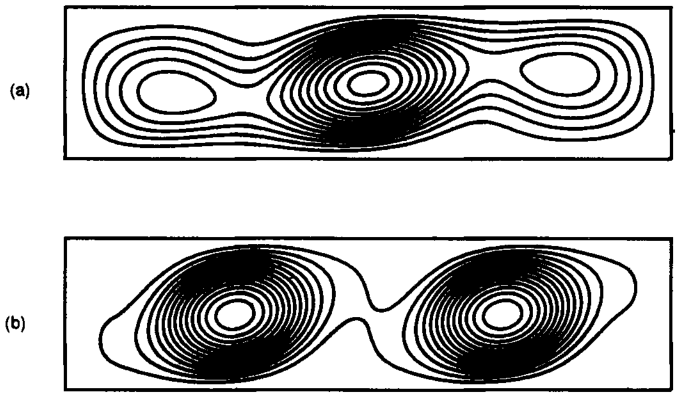

Figure 2. Streamfunction isolines for convection in a melt horizontal layer with side heating: (a) $Gr = 2 \times 10^4$; (b) $Gr = 4 \times 10^4$

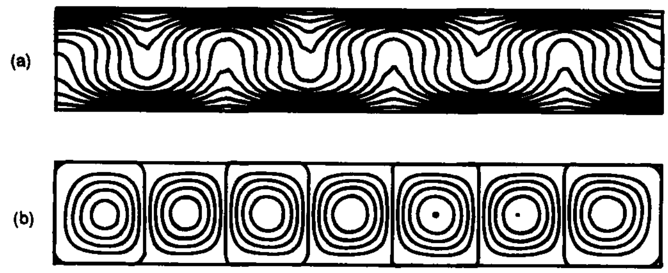

Figure 3. (a) Isotherms and (b) stream function isolines for Rayleigh–Bernard convection in a horizontal layer with bottom heating

a weak supercritical condition. The roll structure of the flat motion and the structure of the temperature field are in a good agreement with the data of other authors (see e.g. Reference 5).

Figures 4–6 show the results of a more difficult problem. In this case the layer is like the one in the previous example. The initial and boundary values for velocity and temperature correspond to the steady state solution shown in Figure 3. The layer begins to slowly rotate with a non-dimensional angular velocity $\Omega L^2/\nu = 20$. All the above-mentioned convective regimes (side heating, bottom and top heating) are changed during the slow rotation. The time dependence of the temperature at a point inside the melt ($x = 1$, $y = 0{\cdot}5$) is shown in Figure 4. One can see transition and quasi-steady regular oscillatory regimes. Streamfunction isolines and isotherms at four instantaneous positions of the layer ((a) bottom, (b) right-side, (c) top and (d) left-side heating) are shown in Figures 5 and 6 respectively. They demonstrate one of the strong effects of slow rotation, namely homogeneity of the temperature field along the layer owing to mixing with different kinds of convection interaction.

This effect is similar to mass transfer in liquid phase epitaxy (LPE) growth problems and has been studied in Reference 10. The possibility of reducing inhomogeneities of a thin film on a substrate in the LPE technique by slow rotation is one alternative to microgravity (mechanical) control (see Reference 18 for more detailed explanations). Slow rotation is also very popular in life science experiments (demonstrations) for imitation microgravity conditions.

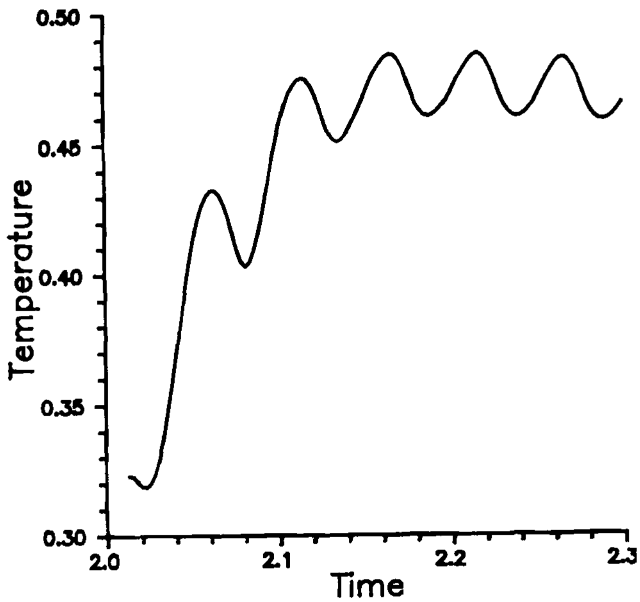

Figure 4. Time dependence of the temperature at a point ($x=1$, $y=0{\cdot}5$) inside the slowly rotated layer, showing the settlement of regular oscillations

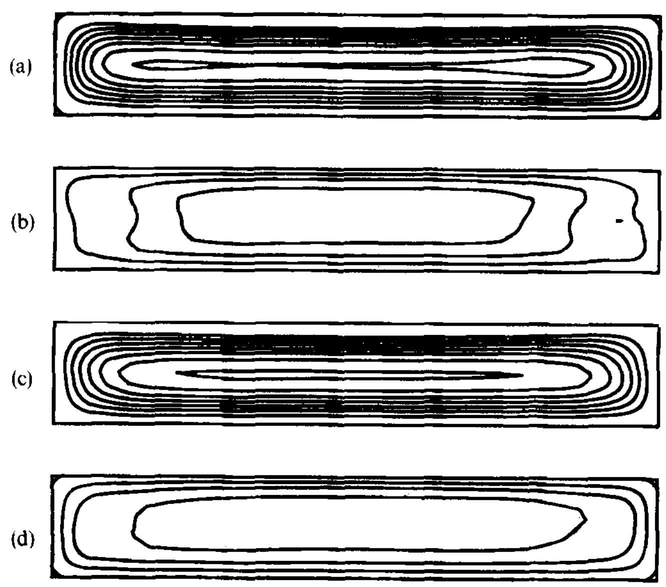

Figure 5. Streamfunction isolines in the slowly rotated layer

The system models a lot of similar situations (with double diffusion, for different types of disturbances, with interaction of gravitational and Marangoni convection,[10, 15] for different kinds of boundary conditions) which can be useful for analysis of material science experiments. Therefore this system can be considered as a powerful 'knowledge base'.

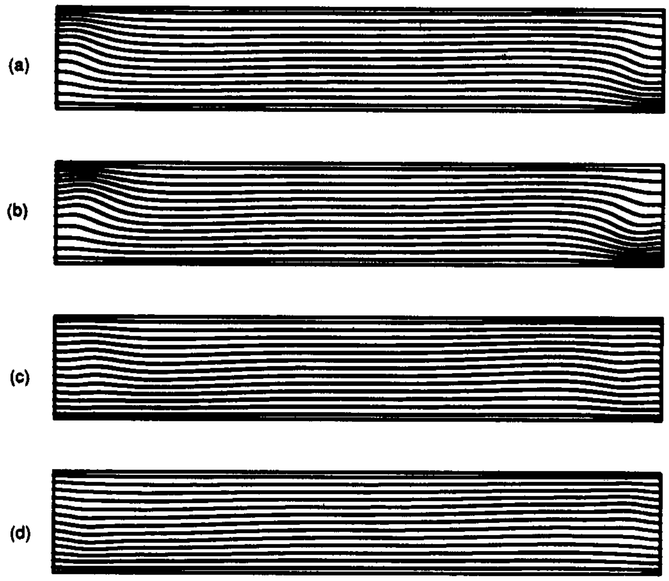

Figure 6. Isotherms in the slowly rotated layer

5. EXAMPLES OF CIVIL AND BUILDING ENGINEERING PROBLEMS

Figure 7 shows the calculation results for a thermal insulation problem (ordinary medium, air, $Ra = 5 \times 10^4$, $Pr = 0{\cdot}71$ (a); permeable porous layer ($Ra^* = 2{\cdot}5$) for isotropic (b) and anisotropic (c, $K_x/K_y = 1500$) media). A 21×51 mesh is used for this problem. The heat transfer across the elements of thermal insulation can be analysed with the help of this system. Thermal convection in the air in an enclosure (Figure 7(a)) is the reason for heat loss from the elements of buildings. It is possible with the help of isotropic permeable porous insulation to reduce the heat loss across the layer (Figure 7(b)) so that the isotherms are close to the conductivity regime and very slow convection exists inside the layer. However, if the permeability is not uniform (the layer is more permeable along and less permeable across), the convection will be more intensive, as shown in Figure 7(c).

Unsteady mixed thermal gravitational and forced convection in a square with input of hot and cold gas and output of mixture as shown in Figure 8 ($Re = 4 \times 10^3$, $Ra = 2 \times 10^7$, $Pr = 1$) has been investigated. A 40×40 mesh is used for this problem. Boundary conditions for velocity and temperature of the input gas (Figure 8) are of the first kind (prescribed u_i and T_i). Conditions for the output gas are of the second kind ($\partial u_o/\partial n = \partial T_o/\partial n = 0$, where n is the normal to the boundary).

6. CONCLUSIONS

The described PC-based system includes repeated and newly tested convective problems in enclosures. The system may be used in addition to engineering handbooks in a number of applications, e.g. material and fluid sciences, thermal insulation and other thermal problems for ordinary and porous media in enclosures for power, civil and building engineering. The system includes a user guide and may be obtained from the authors.

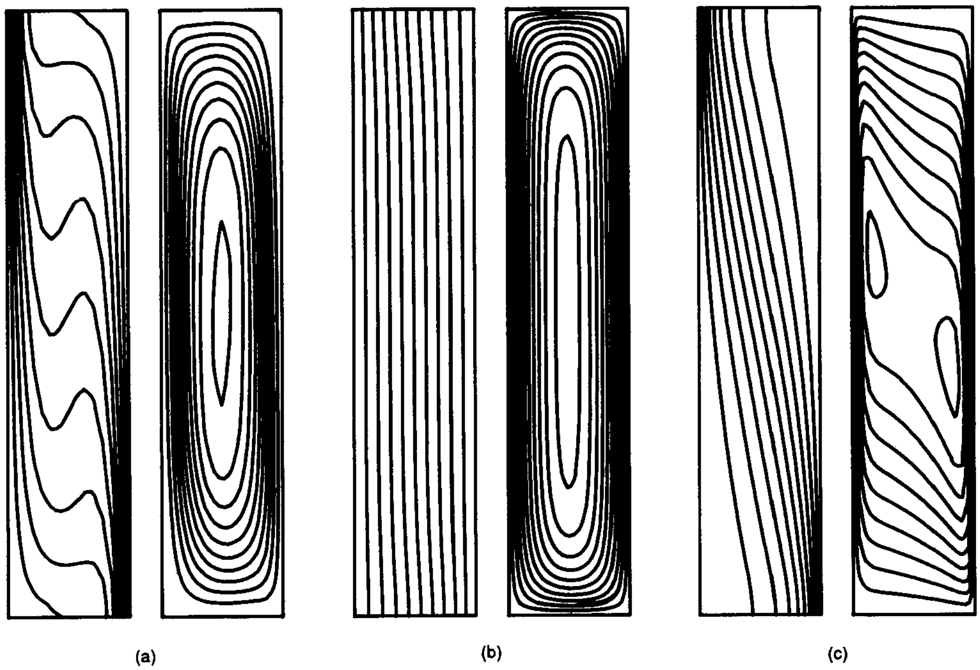

Figure 7. Isotherms (left) and streamfunction isolines (right) for convection in a vertical layer with side heating for (a) ordinary (b) isotropic (c) anisotropic media

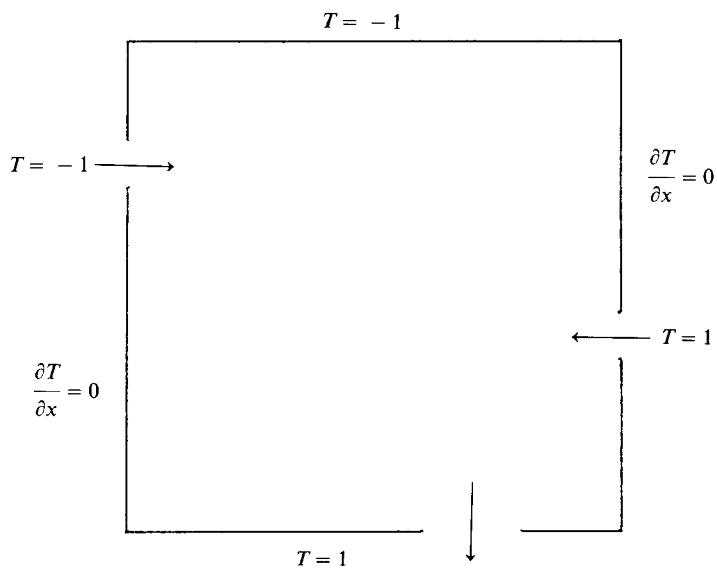

Figure 8. Problem statement for unsteady mixed convection in a square

REFERENCES

1. V. I. Polezhaev, 'Flow and heat transfer for laminar natural convection in a vertical layer', *Trans. 3rd All-Union Conf. on Heat and Mass Transfer*, Minsk, 1968, Vol. 1, pp. 631–640 (in Russian).
2. V. I. Polezhaev, 'Flow and heat transfer with natural convection of a gas in a closed region after loss of hydrostatic equilibrium stability', *Izv. Akad. Nauk SSSR, Mekh. Zhidk. Gaza*, **3**, (5), 124–129 (1968).
3. V. I. Polezhaev, 'Unsteady laminar thermal convection in a closed region with a prescribed heat flux', *Izv. Akad. Nauk SSSR, Mekh. Zhidk. Gaza*, **5**, (4), 109–117 (1970).
4. A. G. Kirdyashkin, V. I. Polezhaev and A. I. Fedyushkin, 'Thermal convection in horizontal layer during side heating', *Izv. Akad. Nauk SSSR, PMTF*, **6**, 122–128 (1983).
5. V. I. Polezhaev and A. I. Fedyushkin, 'Hydrodynamical effects of concentrational segregation in closed region', *Izv. Akad. Nauk SSSR, Mekh. Zhidk. Gaza*, **3**, 11–18 (1980).
6. A. G. Daikovskii, V. I. Polezhaev and A. I. Fedoseev, 'Investigation of the structure of transition and turbulent convection conditions in a vertical layer', *Izv. Akad. Nauk SSSR, Mekh. Zhidk. Gaza*, **6**, 66–75 (1978).
7. M. P. Vlasuk and V. I. Polezhaev, 'Investigation of the heat transfer by natural convection in permeable porous media', *Heat Mass Transfer*, **1**, (2), 140–143 (1972) (in Russian).
8. S. D. Egorov and V. I. Polezhaev, 'Convective heat transfer in anisotropic porous vertical layers', in *Problems in Mechanics and Heat Transfer in Space Technics*, Mashinostroenie, Moscow, 1982, p. 232–241 (in Russian).
9. B. Gebhart, Y. Jaluria, R. L. Mahajan and B. Sammakia, *Buoyancy-induced Flows and Transport*, Hemisphere, New York, 1988.
10. V. I. Poleshaev, A. V. Bune, N. A. Verezub, G. S. Glushko, V. L. Gryaznov, K. G. Dubovik, S. A. Nikitin, A. I. Prostomolotov, A. I. Fedoseev and S. G. Cherkasov, *Mathematical Modelling of Convective Heat and Mass Transfer on the Basis of Navier–Stokes Equations*, Nauka, Moscow, 1987 (in Russian).
11. *Phoenics (Parabolic, Hyperbolic or Elliptic Numerical Integration Code Series)*, Version 1.62, T. M. CHAM.
12. *FIDAP (Fluid Dynamics Analysis Package). Revision 5·0*, Fluid Dynamics International Incorporation, 1989/1990.
13. V. P. Khomenko and G. G. Farenjuk, *Handbook on Thermoinsulation of Buildings*, Budivelnik, Kiev, 1986 (in Russian).
14. R. Peyret and T. D. Taylor, *Computational Methods for Fluid Flow*, Springer, New York, 1982, p. 160.
15. V. L. Grjaznov, M. K. Ermakov, S. A. Nikitin and D. S. Pavlovsky, 'Solving convection problems on a personal computer', *Preprint 481*, Institute for Problems in Mechanics, Moscow, 1990 (in Russian).
16. G. de Vahl Davis, 'Natural convection of air in a square cavity: a bench mark numerical solution', *Int. j. numer. methods fluids*, **3**, 249–264 (1983).
17. B. Roux (ed.), *Numerical Simulation of Oscillatory Convection in Low-Pr Fluids, Notes on Numerical Fluid Mechanics*, Vol. 27, Vieweg, Braunschweig, 1990.
18. V. I. Polezhaev and N. A. Verezub, 'Liquid phase epitaxy: modelling and space experiments', *AIAA Paper 92-0601*, 1992.